J Fluoresc (2015) 25:631–639
DOI 10.1007/s10895-015-1546-9

ORIGINAL PAPER

Enhance Efficiency of Solar Cell Using Luminescence PbS Quantum Dots Concentrators

S. M. Reda

Received: 12 December 2014 / Accepted: 23 February 2015 / Published online: 5 March 2015

Abstract Thin film and sheet PbS quantum dots (QDs) concentrators were synthesized by sol–gel method using three different PbS concentrations (0.14, 0.2, and 0.4 mol %). The structure and morphology of the prepared PbS QDs were characterized by X-ray diffraction (XRD), Scan electron microscopy (SEM), and Transmission electron microscopy (TEM). The photostability of the PbS QDs concentrators under outdoor exposure to sunlight for 8 weeks was studied. The results showed that the PbS QDs sheet with PbS concentration (0.14 mol %) has the highest luminescence intensity. The sheet PbS QDs concentrator was used to couple with PV solar cell and the corresponding photoelectric conversion efficiency was measured under sun light illumination. I–V characteristics of the photovoltaic devices, both open circuit voltage and short circuit current were improved as compared to the device without collector. This indicates that the proposed technique is very useful for improving the efficiency of solar cell.

Keywords PbS quantum dots · Luminescence solar concentrator · Sol–gel · PV cell

Introduction

Renewable energy generation is held back by the high costs (compared to coal and oil) and by the lack of availability of renewable energy sources at all times. While using a power grid can greatly alleviate the latter drawback, the cost of generation still makes it impractical from an economical standpoint to make a massive move towards renewable energy. The price of harnessing solar energy is greatly influenced by the price of the device used to convert solar radiation into electricity – the photovoltaic (PV) cell. These devices typically consist of a semiconductor p-n junction, where solar radiation creates an electron–hole pair that is then separated by a built-in electric field from the depletion zone and transported to the external load. Since the time of their first use for energy generation in 1954 [1], the advances in design and manufacturing processes have reduced the expenses involved. However, even today, the price of generating solar energy remains greater than that of non-renewable power sources. One way to drive down the price of solar energy is to use imaging devices, such as lenses or mirrors, to concentrate solar power onto a small area PV cell. This method, called concentrated photovoltaics (CPV), has the advantage of driving down the cost by reducing the amount of PV required, but due to the nature of the optics used it requires solar tracking and due to limitations of the PV cell's efficiency, can cause overheating that leads to a drop in performance.

An alternative solar energy harvester was proposed in the 1970's, the luminescent solar concentrator (LSC) [2]. In the LSC, sunlight penetrates the top surface of an inexpensive plastic or glass waveguide. This light is absorbed by luminescent molecules which are either embedded in the waveguide or applied in a separate layer on top or bottom of the waveguide. The luminescent molecules can be organic fluorescent dyes, or inorganic phosphors or quantum dots. The absorbed light is re-emitted at longer wavelengths, and a fraction of the re-emitted light is trapped in the waveguide by total internal reflection and becomes concentrated along the edges of the plate. Small PV cells attached to edges of the waveguide collect the emission light and convert it to electricity. Figure 1 shows a cross sectional diagram of an LSC and illustrates the operation of the device.

The LSC has potential advantages over silicon-based PV panels, especially in the built environment. For one, they can

S. M. Reda (✉)
Chemistry Department, Faculty of Science, Benha University, Benha, Egypt
e-mail: safinaz.abdelmotaleb@fsc.bu.edu.eg

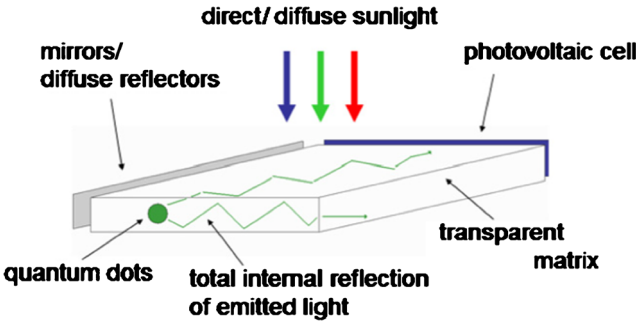

Fig. 1 Schematic illustration of a QD-LSC

reduce the size of the PV cells more than 90 % and the materials for making LSCs are inexpensive, reducing module prices. The plastic waveguide is lighter than the silicon PV panels, leading to a reduction in weight, which makes LSCs more viable for mounting to the sides of buildings. Sunlight can better penetrate the surface of the LSC waveguide from all angles, making them more appropriate for collecting non-direct sunlight. Lastly, LSCs have a great flexibility in design, which make them attractive for architects: they may be made thin and can be cut in any desired shape, cast in almost any color and may be transparent. Since LSCs can be thin, it becomes possible to make curved device. If the photon in/ photon out efficiency is high enough, the cost of electricity generated by the LSC could be competitive [2]. The development of this promising concentrator was limited by the stringent requirements on the luminescent dyes, namely high QE, suitable absorption spectra and red-shifts and stability under illumination [3]. In the past few years, many approaches involving Quantum dots materials have been proposed to improve efficiency of LSCs. In a quantum dot solar concentrator (QDSC) [4] the luminescent species are QDs. QDs have some potential advantages over organic dyes; i.e., the ability to tune the absorption threshold simply by the choice of dot diameter, and being crystalline semiconductors, QDs are more stable and less degradable than organic dyes [3].

Semiconductor quantum dots, also known as nanocrystals or nanoparticles, are a special class of materials whose crystals are composed of periodic groups of II-VI, III-V, or IVVI materials [5]. The most notable and interesting property of semiconductor nanoparticles is the distinct large magnitude change in optical properties as a function of particle size. The three-dimensional quantum-size effect, leading to an increase in band gap with a decrease in particle size, is well known for colloidal semiconductor sols where the individual colloidal particles are dispersed in a liquid or glass [6]. Narrow band gap semiconductor nano-crystals embedded in dielectric matrices, polymers or glass, were observed to behave as quantum boxes when their radii are smaller than their exciton Bohr radii, the circumstances under which their optical properties are strongly modified compared to bulk [7]. Semiconductor quantum dots exhibit significant optical and electronic properties, which can be tuned according to their size. They are strongly luminescent [7], with various possibilities of preparation methods to control their size. It is clear that these semiconductor QDs are promising alternatives to molecular species for luminescence applications [8, 9]. Possible semiconductor QDs include CdS, CdSe, CdTe, $CuInS_2$, Cu_2S, PbS, PbSe, InP, InAs, Ag_2S, Bi_2S_3,Sb_2S_3 and organo lead halide perovskite, which have been used as light harvesters in photovoltaic devices [6, 10]. The synthesis QDs of semiconducting metal sulfide has been an intense field of research due to the interesting properties and potential applications of those compounds [11]. Among sulfides, lead sulfide (PbS) has been investigated along the time because of their optical and electronic properties, what make them suitable for photovoltaic devices [11, 12]. Bulk PbS (rock-salt crystal structure) is a direct band gap IV-VI semiconductor with a narrow band gap of ~ 0.41 eV [11] and a large exciton Bohr radius of ~18 nm at room temperature, which means the strong quantum confinement regime is easily obtained in PbS nanoparticles [11]. The size, shape, capping material and surface characteristics have strong influence on the optical properties of the PbS nanoparticles [13]. PbS QDs have broad absorption spectra with high absorption coefficients facilitating extensive utilization of the solar spectrum and emission peaks that can be tuned from 850 to 1900 nm [11]. Therefore, PbS QDs will present great potential for use as emitters in LSC devices.

A number of methods to synthesize QDs semiconductor nano-crystals have been employed and these include hydrothermal synthesis [14], hydroxide precipitation, chemical bath [11], solid state reactions, spray pyrolysis, laser-heated evaporation, combustion synthesis and the sol–gel technique [15]. Among these methods, sol–gel processing offers many advantages which include low processing temperature, high purity, molecular level homogeneity and more flexibility in the components of the glass [15]. Due to its advantages, the sol–gel approach was used in this study. PbS nanoparticles were incorporated in SiO_2 by a sol–gel process resulting in a nanoparticulate phosphor (nanophosphor) that can be used as QDs LSCs. SiO_2 has been a preferred host matrix for PbS nanoparticles lately because it has been reported to exhibit high fluorescence intensity compared to other matrices [15].

In this study PbS QDs in thin film and sheet form were prepared by sol–gel method. The effect of concentration of PbS on the optical properties of QDs were investigated to verify the potential use of this kind of composite for LSC applications.

Experimental

Preparation of PbS QDs

SiO_2: PbS gel was prepared by mixing 10 ml of tetraethylorthosilicate (TEOS) (Aldrich) solution, 5 ml of

ethanol (EtOH), and 5 ml of 0.15 M nitric acid (HNO_3). The mixture was stirred at room temperature for 1 h. The mixture of 0.03 g of $Pb(CH_3COO)_2.3H_2O$ (Aldrich) dissolved in 5 ml of ethanol "0.14 mol%" and 0.01 g of Na_2S (Aldrich) dissolved in 5 ml of ethanol were add to the above solution dropwise with continuous stirring for 30 min. The gel was allowed to dry at room temperature for ~10 days, crushed into sheets and annealed in air at 200 °C for 2 h. The obtained sheet has a dimension of $2\times1\times0.5$ cm^3.

The spin coating technique was used to fabricate thin film PbS QDs using the prepared sol on cleaned quartz glass substrates with speed (900 r.p.m). The as-deposited film was annealed in air at 200 °C for 2 h.

The same method was used to prepare thin film of SiO_2: PbS with PbS concentration 0.2 and 0.4 mol%.

The overall equation for the formation of PbS from the solution of $Pb(CH_3COO)_2.3H_2O$ and Na_2S is [16];

$$Pb\,(CH_3COO)_2.3H_2O + Na_2S \rightarrow PbS + 2Na^+ + 2CH_3COO^- + 3H_2O.$$

Characterization of PbS QDs Embedded SiO_2 Matrix

The lead sulphide (PbS) in the amorphous SiO_2 matrix was characterized using X-ray diffraction, Scan electron microscope (SEM) and Transmission electron microscope (TEM). X-ray diffraction (XRD) study was carried out on a Diano Corporation USA diffractometer using Co radiation (k=0.179 nm). SEM and TEM were taken by an electron microscope model JEM-5200 Jeol and Joel 2010, respectively.

Outdoor testing was carried out for 8 weeks in (summer 2014), March, April in Benha city, Egypt. Absorption spectra were recorded using a Perkin–Elmer Lambda 40 spectrophotometer in wavelength range (200–900 nm) at room temperature. Fluorescence spectra have been recorded using the Jasco FP777 spectrofluorometer.

Photovoltaic Cell Coupled with PbS QDs LSC

The PbS QDs LSC with dimensions of $2\times1\times0.5$ cm^3 was used to couple with a commercial Si solar cell of dimensions ($2\times1\times0.5$ cm^3). LSC was placed over the top of PV cell. The efficiency of cell was measured before and after coupling with the PbS QDs LSC under direct sunlight illumination intensity of 1000 W/m^2 on June (2014). The open-circuit voltage (V_{oc}) and the short-circuit photocurrent (J_{sc}) were measured using Voltameter Keithley Model 175 A and Electrometer Keithley Model 614 A, respectively.

Results and Discussion

Characterization of PbS QDs

X-ray diffraction spectrum of PbS QDs thin film and sheet at different concentrations of PbS embedded in SiO_2 matrix are shown in Fig. 2. This figure shows broader peak widths of the PbS nanoparticles. The broadening of the peaks is attributed to small crystallites or nanocrystalline nature of the PbS (particle size effect). This figure shows also that as the concentration of PbS increases, the intensity of the peaks increases and the width of the peaks decreases. The six diffraction peaks of PbS at 2θ=(28°), (32°), (43°), (51°), (58°) and (68°) correspond to the (111), (200), (220), (311), (222) and (400) planes, respectively. These diffraction planes can be indexed to the cubic phase of PbS [15]. The Figure shows the broad peak at 25° corresponds to the typical diffraction of amorphous SiO_2 (Si-O short-order structure) [15].

The Debye-Scherrer's equation [15],

$$D = \frac{0.94\lambda}{\beta cos\vartheta} \quad (1)$$

was used to determine the average size (D) of the PbS with the full-width at half-maximum of the diffraction peaks (β), λ the X-ray wavelength (0.179 nm). The nanocrystallite size was calculated from the broadening of the (111) plane and are listed in Table 1. It was found that the crystallite size of PbS increases from 10.5 to 16.8 nm as the concentration of PbS increases from 0.14 to 0.4 mol%. By increasing the PbS concentration, the growth of larger QDs using the same annealing procedures might be expected. The main reason for this behaviour is the decreasing distance between Pb^{2+} and S^{2-} ions as the concentration increases [8].

The surface morphology of thin film and sheet PbS QDs were observed through SEM image analysis and these

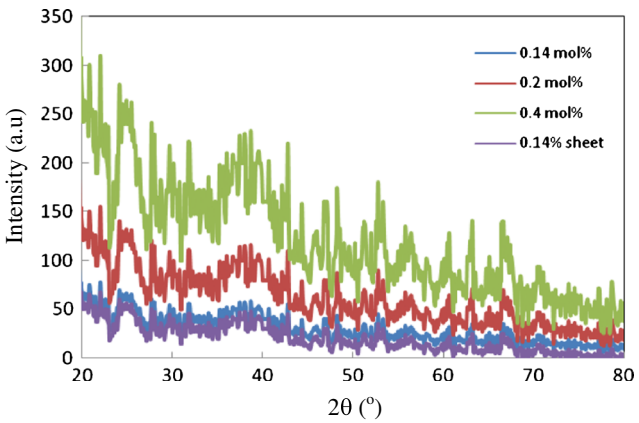

Fig. 2 X-ray spectra of PbS QDs embedded in silica matrix in thin film and sheet form

Table 1 Particle sizes (D_{XRD}, D_{TEM}, $D_{optical}$) and optical parameters, such as absorption band gap (E_g), absorption peak position (λ_{ab}), photoluminescence peak position (λ_{em}), Stokes shift ($\Delta\lambda$), percentage of optical density (P%) for PbS QDs embedded in silica matrix

Sample	D_{XRD} (nm)	D_{TEM} (nm)	$D_{optical}$ (nm)	E_g (eV)	λ_{ab} (nm)	λ_{em} (nm)	$\Delta\lambda$ (nm)	P%
Sheet (0.14 %)	10.7	10.3	10.5	1.70	653	830	177	84.5
Thin film (0.14 %)	10.5	10.2	10.1	1.72	650	839	189	70.1
Thin film (0.2 %)	11.6	11.3	11.5	1.66	677	839	162	79.4
Thin film (0.4 %)	16.8	16.1	16.5	1.60	705	839	134	88.8

micrographs are given in Fig. 3. Figure 3a shows that average grain size in the obtained PbS thin film and sheet with concentration (0.14 mol %), in which almost spherical-like PbS nanoparticles are observed. Figure 3b and c shows that the film has islands with different size and shapes, whose distributions on the surface are almost uniform. Among the islands, sparsely distributed hollow sites can be observed. Increasing concentration of PbS results in a decrease in the size of the islands, whereas the hollow sites get smaller and sparser. Thus, denser and more homogeneous films could be produced by increasing concentration.

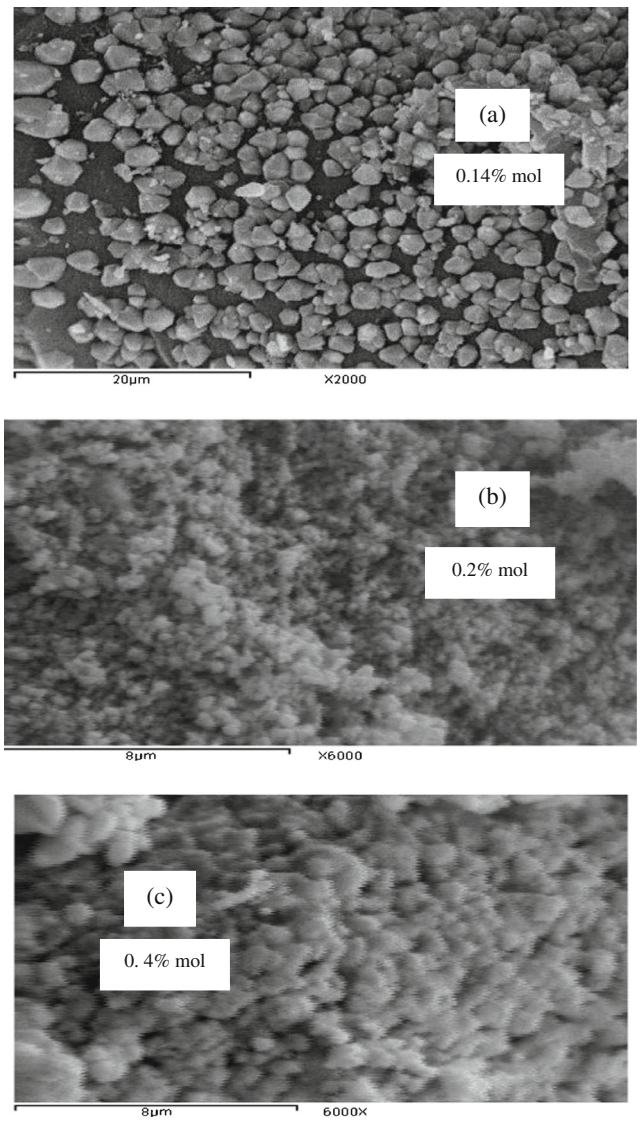

Fig. 3 SEM micrograph of PbS QDs embedded in silica matrix: (**a**) sheet; (**b**, **c**) thin film with different concentrations

Figure 4 illustrates the TEM image of PbS QD embedded SiO_2. In the images, a large number of PbS QDs are formed in the glass matrix. The morphology of QDs nanophosphors is rod-shaped and the average size of these rods is between 10.3 and 16.1 nm, which in accordance with the X-ray results, Table 1. This size is smaller than the Bohr radius of the bulk exciton (18 nm), which necessary to expect a quantum confinement effect. It is, clear from Fig. 4b and c that the larger particles are made up of agglomeration of smaller particles by increasing concentration. The relatively large size of PbS QDs is probably due to the high doping concentration of PbS in amorphous SiO_2 preparation, which results in the inhomogeneous migration of S source and growth of PbS nuclei during PbS QD formation.

Optical Studies

Figure 5 shows the absorption spectra of PbS QDs LSCs. This Figure shows that for the as-prepared samples, PbS QDs absorb larger wavelength range of photons. These broad absorption peaks were directly related to the formation of PbS nanocrystals. The broad absorption bands were formed at the wavelengths of 650, 677 and 705 nm for PbS thin films prepared with concentration 0.14, 2 and 4 mol%, respectively. The red shift of the absorption band of PbS QDs thin film confirms that the size of PbS QDs grows continuously with the increase of concentration. This result agrees with that obtained from X-ray measurements. The intensity of the absorption band is also enhanced with the increase of concentration. This indicates that the number density of PbS QDs in silica matrix also increases when the concentration increases from 0.14 to 4 mol%. Figure 5 shows that there is no change in the position of absorption band by change shape of PbS QDs LSC with the same concentration (0.14 mol %). This indicates the stability of this kind of QDs and can be used as LSC in different form.

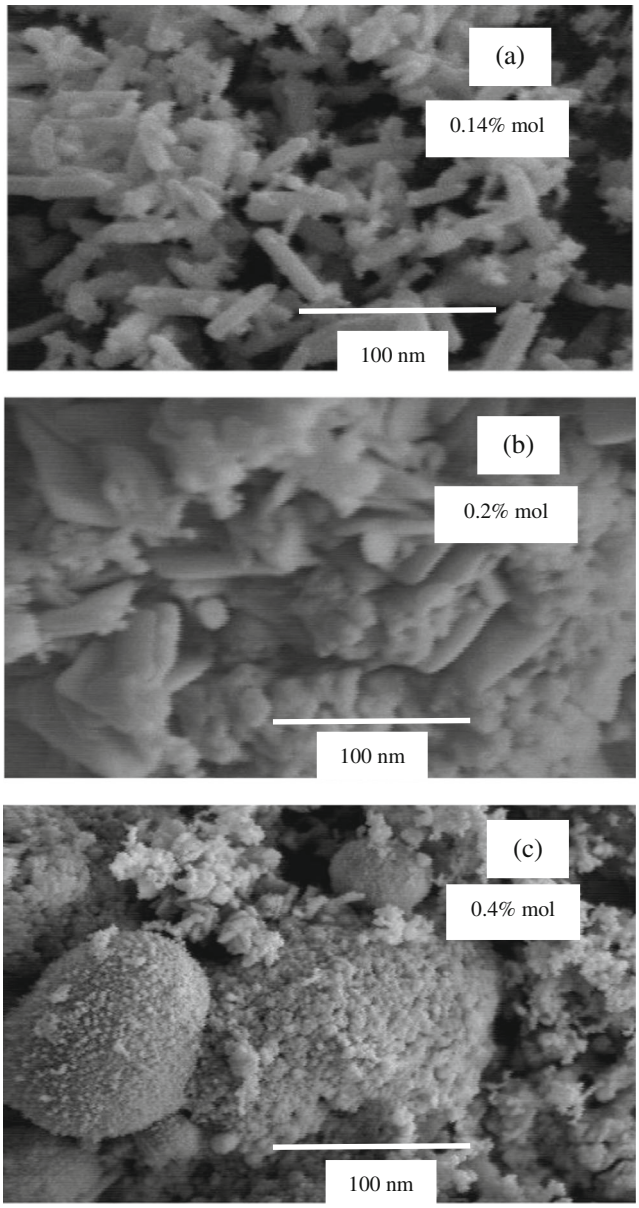

Fig. 4 TEM picture of PbS QDs embedded in silica matrix: (**a**) sheet; (**b**, **c**) thin film with different concentrations

The optical band gap (E_g) of the PbS QDs was calculated using the relation:

$$(\alpha E) = A\left(h\nu - E_g\right)^n \quad (2)$$

where α is the optical absorption coefficient derived from the absorption data, hν is the photon energy and A is a constant. The index n has discrete values such as 1/2, 3/2, 2 or higher depending on whether the transition is direct or indirect and allowed or forbidden. In the direct and allowed cases, the index n is 1/2, whereas for the direct but forbidden cases it is 3/2. But for the indirect and allowed cases $n=2$ and for the forbidden cases it is 3 or higher. The plots of $(\alpha E)^2$ versus photon energy (hν) showed linear behavior for $n=1/2$, Fig. 6. From extrapolating the straight line to zero photon energy the values of the band gaps energy are calculated and listed in Table 1. From this Table there is a clear blue-shift in the values of the optical band gap from bulk PbS. The observed blue-shift of the E_g with respect to bulk may be attributed to the interaction of the PbS nanocrystallites with SiO_2 at their interfaces. During deposition, the PbS experience sulfur (S) loss due to an outward diffusion process, and as a result there is expected to be large density of S vacancies in the sample. Eventually this leads to a decrease in the band gap due to disorder effects produced by S vacancies and Pb interstitial defects. In contrast, an amorphous semiconductor has a tail in the absorption spectrum encroaching into the empty band gap. Since the band gap of the semiconductor in the nano-scale regime is tunable, the decrease in the band gap could be attributed to this band tail effect caused by the impurities in the sample. The nature of the localization of electrons and holes in a confined space which results in quantum size effect demands electronic isolation between particles. When individual particles are in electrical contact, they might lose their quantization effect. Table 1 shows also that there is a clear blue-shift in the values of the optical band gap of PbS thin film with increasing concentration. The change in E_g with the concentration is attributed to quantum confinement effect

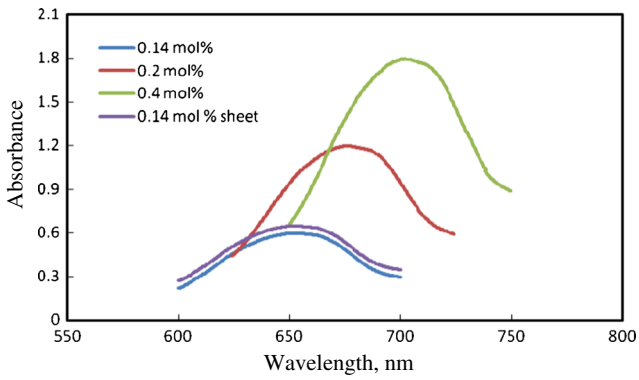

Fig. 5 Absorption spectra of PbS QDs LSCs in different forms

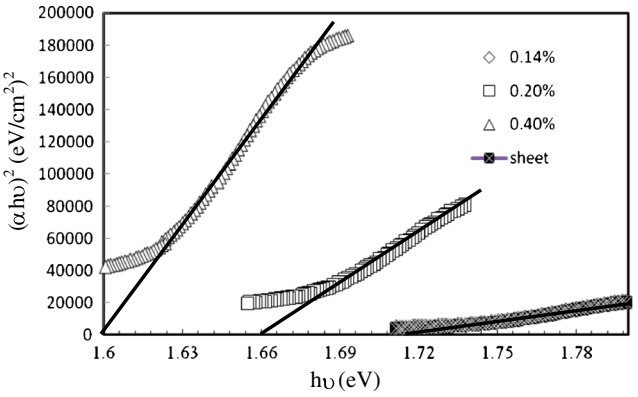

Fig. 6 Plot of $(\alpha h\nu)^2$ vs. hν of PbS QDs LSCs in different forms

[15]. The blue-shift of the band gap energy of the film is also believed to originate from the residual stress in the film due to lattice distortion [11].

According to previous works, the average size of PbS QDs in SiO_2 matrix can be estimated by the following equation [8],

$$\left(E_g(R)\right)^2 = E_g^2 + \left(\frac{2\hbar^2 E_g}{m^*}\right)\left(\frac{\pi}{R}\right)^2, \quad (3)$$

where R is the average radius of PbS QDs, ħ is Planck's constant, m* is the effective mass of electron, $E_g(R)$ is the effective energy of PbS QDs, and E_g is the band gap energy of bulk PbS semiconductor. For bulk PbS semiconductor, E_g=0.41 eV and $m^*=0.085m_e$, where m_e is the static electron mass [8]. Since PbS is a direct bandgap semiconductor, the effective energy of PbS QDs can be evaluated by the fitting of the absorption spectra [8] and are listed in Table 1. It is clear from Table 1 that there is an increase in the values of the average radius with increasing concentration of PbS in thin film form. Also the PbS QDs in thin film and sheet form with the same concentration has the same radius. The values obtained via this method match well with that were calculated from XRD and TEM.

Figure 7 shows the photoluminescence (PL) spectra of PbS QDs in thin film and sheet form. PL emission spectrum of PbS QDs in sheet form showed a broad peak at ~ 814 nm. The PL band covers the wavelength from 750 to 850 nm, with a full width at half maximum (FWHM) of 60 nm. This emission is attributed to PbS nanoparticles in SiO_2, which is in good agreement with other published PL spectra of PbS particles [17]. The PL emission from the PbS sheet is more intense than that of the thin film made from the same concentration. The weak PL intensity of the film is attributed to some incidental defects that could have been introduced in the thin film during preparation process. The PL spectrum of the thin film is red-shifted from that of the sheet by approximately 9 nm. The red-shift is ascribed to band tail effects [8] associated with incidental impurities/defects in the material. The FWHM also broadens to 120 nm. The large FWHM was probably induced by the large size dispersion of PbS QDs in silica.

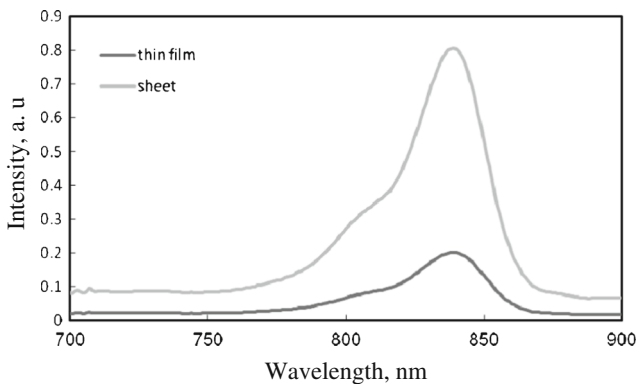

Fig. 7 PL spectra of PbS QDs LSCs in sheet and thin film form with concentration 0.14 mol %

Figure 8 shows the PL spectra of PbS QDs thin film with concentration of PbS varied from 0.14 to 0.4 mol%. Spectra show that with an increase in PbS concentration, the shapes and positions of the emission peaks show no obvious changes. The PL emission intensity of PbS increases with the increase in the mole concentration of PbS and reached the maximum at the concentration of 0.2 mol%. Further increase in the PbS concentration (beyond 0.2 mol %) resulted in the decrease in the PL intensity. This suggests that the emission center of PbS is quenched at high concentration. So that, we prefer lower concentration in preparing LSCs from PbS QDs.

The Stokes shift (Δλ), which is the difference between the wavelength at which the absorption and emission maxima are observed, is presented in Table 1. It can be seen that Stokes shift of thin film PbS QDs is higher than sheet with the same concentration. These large Stokes shift was most probably induced by the defects on the surface of PbS QDs. This would lead to a decrease of the re-absorption losses in a LSC [3]. By increasing concentration of PbS in the thin film the Stokes shift deceases. Hence, the lowest concentration is preferable in fabrication of high-efficiency PbS QD solar concentrators. It is reasonable to expect a change in the overall efficiency of a luminescent solar concentrator when this optimized PbS concentration is used to fabricate the luminescent solar concentrator, as the overall optical efficiency mainly depends on the total emission of luminescent species.

Based on the results discussed above, it can be deduced that the formation characteristic of PbS QDs in silica matrix can be widely tuned by controlling the concentration of QDs and shape of concentrator. This will further tune the PL wavelength, Stokes Shift and bandwidth of PbS QD embedded silica, which is significant for the application in broadband luminescent solar concentrators.

Photostability of PbS QDs

The photostability of the PbS QDs samples under outdoor exposure to sunlight for 8 weeks was studied. Figure 9 shows

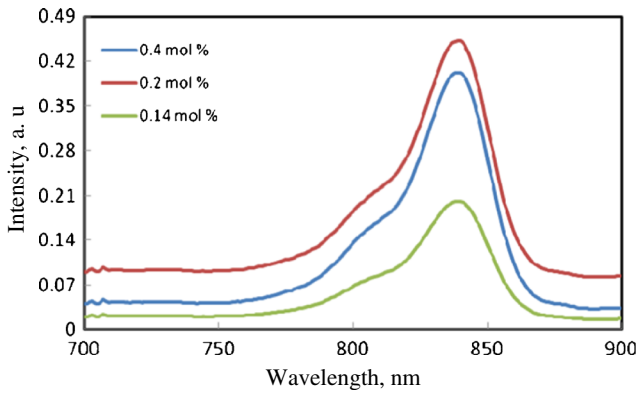

Fig. 8 PL spectra of PbS QDs LSCs thin films with different concentrations of PbS

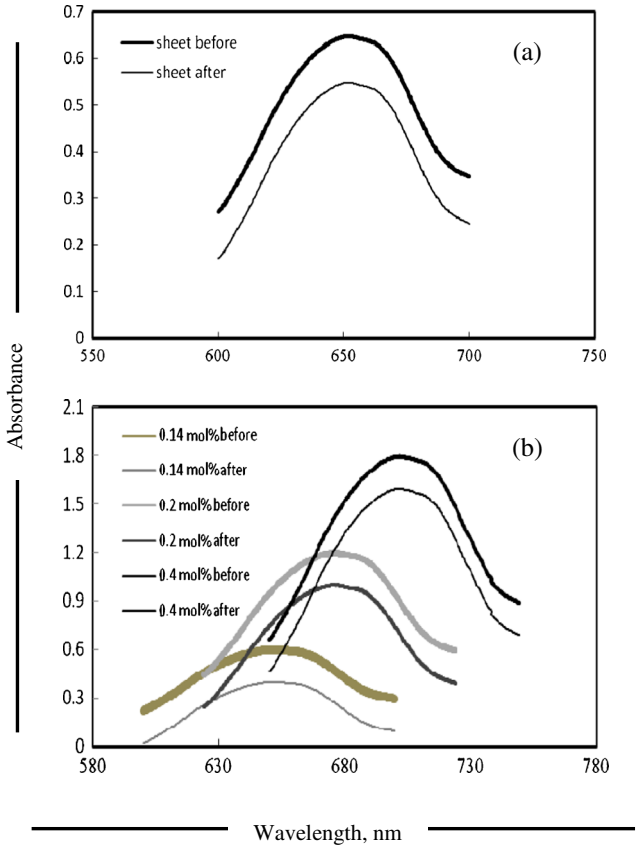

Fig. 9 The change in absorption spectra of PbS QDs LSCs before and after exposure to sun light for 8 weeks in sheet (**a**) and thin form (**b**)

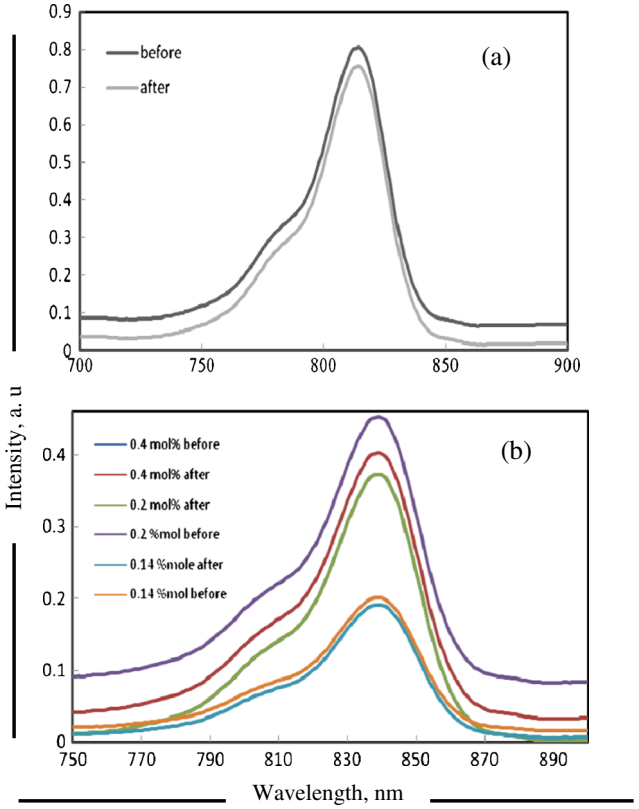

Fig. 10 The change in PL spectra of PbS QDs LSCs before and after exposure to sun light for 8 weeks in sheet (**a**) and thin form (**b**)

that there is no change in shape or position of absorbance peaks. This indicates that the use of quantum dots provides stability against photobleaching under solar irradiation and can be used as highly stable luminescent solar concentrators.

The percentage of optical density changes of the PbS QDs was calculated from the relation [18]:

$$P\% = \frac{A_t}{A_o} X 100\%, \quad (4)$$

where A_t and A_o the maximum absorption after and before illumination, respectively, and P% the percentage of QDs samples remains after 8 weeks. Table 1 shows that thin film sample with concentration 0.4 % and sheet sample with concentration 0.14 % has the highest photostability compared with the others samples. So that, these samples can be selected for field performance of luminescent QDs concentrators.

Photoluminscence Properties

Figure 10 shows the PL of PbS QDs before and after exposure to sunlight for 8 weeks. The samples have significantly different luminescent intensities and there is no change in shape or position of emission peak for all samples with time. Due to the highest luminescence intensity of PbS QDs sheet, this QD can be used for solar concentrator fields. Therefore, the proposed concept of QDs photoluminescent solar concentrators could be very promising regarding the criterion of energy cost.

From the above results we found that PbS QDs in sheet form has the highest PL intensity. So that, we choose this sample as the luminescent solar concentrator to enhance the efficiency of the PV solar cell under direct sun light illumination.

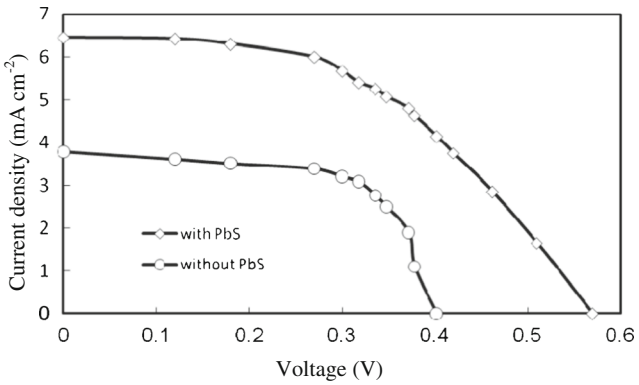

Fig. 11 Current–voltage curves for PV cell with and without PbS QDs LSC in sheet from with PbS concentration 0.14 mol % under direct sun light illumination

Table 2 Summary of the obtained photovoltaic performance parameters from the PV cell before and after coupled with PbS QDs sheet collector with concentration 0.14 %

Sample	J_{sc} (mA.m^{-2})	V_{oc} (V)	J_m (mA.m^{-2})	V_m (V)	FF	PCE%
With PbS collector	6.45	0.57	5.07	0.35	0.47	0.17
Without PbS collector	3.78	0.40	3.08	0.32	0.65	0.09

Photocurrent Measurements

I–V curve of the PV solar cell coupled with PbS QDs collector is shown in Fig. 11. The photovoltaic parameters of the solar cell with and without PbS concentrator are summarized in Table 2. All photovoltaic performance parameters were increased compared to those of the cell without concentrator, with J_{sc} of 6.45 mA cm^{-2}, V_{oc} of 0.57 V, FF of 0.47, and PCE of 0.17 %. The high J_{sc} indicated that a good connection between PbS QDs and the cell. So, we can say that the cell efficiency was greatly improved by coupling with PbS QDs collector. However, the PCE of 0.17 % is still too low for commercial generation purposes. The QDs used in this work only absorb 31 % of the AM1.5G spectrum between 600 and 750 nm that is available to Si cells. To improve the PCE broader absorption up to the near IR would be required in addition to much lower re-absorption losses. Broader absorption could be achieved either by using larger QDs or by changing material system and if re-absorption losses were minimized the device efficiency would be approximately doubled [3]. Therefore broader absorption and emission at wavelengths near the band-gap of Si, together with reduced re-absorption losses, could therefore lead to practical sized devices with PCEs nearing 5 %.

Conclusion

Thin film and sheet luminescent PbS quantum dots concentrators were prepared by sol–gel method using different PbS concentrations. The prepared concentrators were characterized by XRD, SEM, TEM, and optical spectroscopy. It was observed that larger QDs were formed by increasing concentration. Both absorption and PL peaks are observed in the visible region owing to the strong quantum confinement effect. The PbS QDs spectra reveal red-shift when increasing concentration. This shift was due to the changes in the band gap energies induced by concentration. The photostability was carried out under outdoor exposure to sun light at different time. Fluorescence properties showed that the PbS QDs sheet exhibits the highest fluorescent intensity. Therefore this QD concentrator was used to couple with PV solar cell. All photovoltaic parameters were increased compared to those of the cell without concentrator.

Acknowledgments The author wishes to thank all the staff members and my colleagues at Chemistry Department, Faculty of Science, Benha University, Egypt for their cooperation during this work www.fsci.bu.edu.eg.

References

1. Shcherbatyuka GV, Inmana RH, Winston R, Ghosha S (2010) Design and performance of nanostructure-based luminescent solar concentrators. Proc SPIE 7769:1–7
2. Verbunt PPC, Debije MG (2011) Progress in luminescent solar concentrator research: solar energy for the built environment. World Renewable Energy Congress 8:2751–2758
3. Bomm J, Büchtemann A, Chatten AJ, Bose R, Farrell DJ, Chan NLA, Xiao Y, Slooff LH, Meyer T, Meyer A, Sark WGJHM, Koole R (2011) Fabrication and full characterization of state-of-the-art quantum dot luminescent solar concentrators. Sol Energy Mater Sol Cells 95:2087–2094
4. Kennedy M, Mc Cormack SJ, Doran J, Norton B (2009) Improving the optical efficiency and concentration of a single-plate quantum dot solar concentrator using near infra-red emitting quantum dots. Sol Energy 83:978–981
5. Hyldahl MG, Bailey ST, Wittmershaus BP (2009) Photo-stability and performance of CdSe/ZnS quantum dots in luminescent solar concentrators. Sol Energy 83:566–573
6. Roland KPBPJ, Mahabaduge H, Haugen NO, Grice CR, Jeong S, Dykstra T, Gao J, Ellingson RJ (2013) Thin film solar cells based on the heterojunction of colloidal PbS quantum dots with CdS. Sol Energy Mater Sol Cells 117:476–482
7. Mocanu A, Rusen E, Diacon A, Dinescu A (2014) Hierarchical nanostructures of PbS obtained in the presence of water soluble polymers. Powder Technol 253:237–241
8. Dong G, Wu G, Fan S, Zhang F, Zhang Y, Wu B, Ma Z, Peng M, Qiu J (2014) Formation, near-infrared luminescence and multi-wavelength optical amplification of PbS quantum dot-embedded silicate glasses. J Non-Cryst Solids 383:192–195
9. Schüler A, Python M, Valle del Olmo M, de Chambrier E (2007) Quantum dot containing nanocomposite thin films for photoluminescentsolar concentrators. Sol Energy 81:1159–1165
10. Snaith HJ, Stavrinadis A, Docampo P, Watt AAR (2011) Lead-sulphide quantum dots sensitization of tin oxide based hybrid solar cells. Sol Energy 85:1283–1290
11. Göde F, Güneri E, Emen FM, Emir Kafadar V, Ünlü S (2014) Synthesis, structural, optical, electrical and thermoluminescence properties of chemically deposited PbS thin films. J Lumin 147:41–48
12. Shcherbatyuk GV, Inman RH, Wang C, Winston R, Ghosh S (2010) Viability of using near infrared PbS quantum dots as active materials in luminescent solar concentrators. Appl Phys Lett 96:191901
13. Nejo AO, Nejo AA, Pullabhotla RVSR, Revaprasadu N (2012) Facile synthesis of organically capped PbS nanoparticles. J Alloys Compd 537:19–23
14. Goswami SK, Oh E (2014) Morphology control and photovoltaic application of solvothermally synthesized PbS nanostructures. Mater Lett 117:138–141
15. Martucci A, Fick J, Le Blanc S-E' m, Lo Cascio M, Hache A (2004) Optical properties of PbS quantum dot doped sol–gel films. J Non-Cryst Solids 345&346:639–642

16. Swart HC, Terblans JJ, Dhlamini MS (2008) Luminescent Properties of synthesized PbS nanoparticle phosphors. (MSc) thesis. Faculty of Natural and Agricultural Sciences, Department of Physics at the University of the Free State
17. Naves PM, Gonzaga TN, Monte AFG, Dantas NO (2006) Band gap energy of PbS quantum dots in oxide glasses as a function of concentration. J Non-Cryst Solids 352:3633–3635
18. Thiagarajan V, Selvaraju C, Ramamurthy P (2003) Ex-cited state behaviour of acridinedione dyes in matrix: Inhomogeneous broadening and enhancement of triplet. J Photochem Photobiol A Chem 157: 23–31